6.1. SATELLITE- AND GROUND-BASED STEREO ANALYSIS OF CLOUDS

Gabriela Seiz [*], Manos Baltsavias, Armin Gruen
Institute of Geodesy and Photogrammetry, Swiss Federal Institute of Technology (ETH), Zurich

ABSTRACT

In this paper, the possibilities of satellite-based and ground-based stereoscopy of clouds are examined, with the objective to derive cloud-top and cloud-base heights and motion. These parameters are very important for a better description of clouds for nowcasting and numerical weather prediction models.

For the satellite part, coincident images of MISR (on EOS Terra), ASTER (on EOS Terra) and ATSR2 (on ERS-2) are used. For the ground-based part, stereo images from our newly developed imager system are used. The cameras were installed during the Mesoscale Alpine Programme (MAP) in the target area 'Rhine Valley' in October 1999 and at Zurich-Airport, Switzerland, in September 2001 and April 2002, in coincidence with overpasses of EOS-Terra and ERS-2.

In principle, the same stereo matching algorithms, based on least-squares matching, are applied on both the satellite-based and ground-based images. With respect to the different spatial resolution of the sensors, the matching strategy has to be adjusted accordingly. Furthermore, the main differences in the processing chain between the satellite-based and ground-based data sets are the geometric calibration of the sensors, the preprocessing procedures and the quality-control algorithms.

Finally, two case studies of coincident ground- and satellite-based retrieval of cloud-base/cloud-top height and motion are presented. The ground measurements with our new stereo camera system showed to be an interesting technique to validate satellite-based cloud-top height and motion of vertically thin clouds and to additionally detect smaller scale cloud features, which is particularly important for accurate nowcasting in mountainous terrain. Furthermore, the 3D results from coincident satellite and ground measurements can be taken as input data for numerical cloud and very high resolution weather models.

1. INTRODUCTION

The European Union (EU-FP5) project Cloudmap2 aims to produce and exploit value-added remote sensing data products on macroscopic (e.g. cloud-top height) and microscopic (e.g. cloud droplet radius) properties and water vapour distributions in order to characterize sub-grid scale processes within Numerical Weather Prediction Models (NWP) through validation and data assimilation. Earth Observation (EO) data, provided by ESA, EUMETSAT and NASA are used to derive geophysical value-added data products over Europe and the North Atlantic region, whenever possible in near real-time. Ground-based active (cloud radar, ceilometer) and passive (stereo imager system, IR camera) remote-sensing instruments are used to validate the EO-derived products as well as to be merged with the satellite-based results for a whole 3D representation of the clouds. Numerical simulation experiments based on radiative transfer methods are used to quantify the effect of broken clouds on the Earth's radiation budget and lead to a better representation of clouds within NWP models.

This paper describes the stereo-photogrammetric results obtained in cloud-top height and wind estimation from satellite sensors using stereo images at various resolutions (ASTER, ATSR2, MISR, Meteosat-6/-7) and spectral wavelengths (ATSR2), the cloud-base height and motion results from the new ground-based stereo imager system, and presents two case studies where the ground- and satellite-based results can be compared.

2. SATELLITE-BASED STEREO ANALYSIS

Stereoscopy of clouds has a long tradition in satellite meteorology (Hasler, 1981). Stereo measurements have the advantage that they depend only on basic geometric relationships of observations of cloud features from at least two different viewing angles, while other cloud top height estimation methods are dependent on the knowledge of additional cloud/atmosphere parameters like cloud emissivity, ambient temperature or lapse rate. From satellites, both geostationary and polar-orbiting sensors can be used in a number of configurations, as described in e.g. Fujita (1982), Campbell and Holmlund (2000), Yi et al. (2001). Over Europe, the following satellite configurations can be used for cloud stereoscopy:

- Single polar-orbiter with two views: ERS2-ATSR2 (ENVISAT-AATSR), EOS Terra-ASTER
- Single polar-orbiter with more than two views: EOS Terra-MISR
- Two geostationary Meteosat satellites: Meteosat-6 and Meteosat-7

Further combinations, like a Meteosat satellite with another geostationary satellite (e.g. GOES-E) or a Meteosat satellite with a polar-orbiter instrument (NOAA AVHRR, ATSR2, MISR, ASTER), are not

[*] Corresponding author address: Gabriela Seiz, Institute of Geodesy and Photogrammetry, ETH-Hönggerberg, 8093 Zürich;
e-mail: gseiz@geod.baug.ethz.ch

recommended due to the S-N scanning direction of the Meteosat satellites (while all other geostationary satellites are N-S scanning). The different scan directions additionally increase the difficulty for the matching and the motion error correction.

2.1 Single polar-orbiter with two views

2.1.1 ATSR2

The ATSR2 instrument is part of the ERS-2 satellite system which was launched in April 1995. The successor sensor, AATSR, is part of Envisat which was recently launched in spring 2002. ERS-2 is in a near-circular, sun-synchronous orbit at a mean height of 780km, an inclination of 98.5 and a sub-satellite velocity of 6.7 km/s. The spacecraft is positioned to operate with a descending equator crossing of around 10:30 local solar time and of a ascending equator crossing of 22:30 local solar time. The repeat cycle is about 3 days. First, the ATSR2 views the surface along the direction of the orbit track at an incidence angle of 55° as it flies toward the scene. Then, some 120s later, ATSR2 records a second observation of the scene at an angle close to the nadir (Mutlow, 1999). ATSR2's field of view comprises two 500 km-wide curved swaths, with 555 pixels across the nadir swath and 371 pixels across the forward swath. The pixel size is 1x1 km at the center of the nadir scan and 1.5 x 2 km at the center of the forward scan. The sensor records in 7 spectral channels: 0.55µm, 0.67 µm, 0.87 µm, 1.6 µm, 3.7 µm, 10.8 µm, 12.0 µm, which is comparable to the channels of the new SEVIRI instrument on MSG. The geolocation for the rectified (GBT) products proceeds by mapping the acquired pixels onto a 512x512 grid with 1km pixel size whose axes are the ERS-2 satellite ground-track and great circles orthogonal to the ground-track.

2.1.2 ASTER

The Advanced Spaceborne Thermal Emission and Relfection Radiometer (ASTER) is an advanced multispectral imager that was launched on board NASA's Terra spacecraft in December 1999 (ASTER, 2002). ASTER covers a wide spectral region with 14 bands from the visible to the thermal infrared with high spatial, spectral and radiometric resolution. An additional backward-looking near infrared band provides stereo coverage. The sensor consists of three separate instrument subsystems: the Visible and Near Infrared (VNIR) has three bands with a spatial resolution of 15 m (named 1, 2, 3N), and an additional backward telescope for stereo (named 3B); the Shortwave Infrared (SWIR) has 6 bands with a spatial resolution of 30 m; and the Thermal Infrared (TIR) has 5 bands with a spatial resolution of 90 m. Each ASTER scene covers an area of 60 x 60 km.

The VNIR subsystem, which provided the used 3N/3B stereo images, consists of two independent telescope assemblies to minimize image distortion in the backward and nadir looking telescopes. The detectors for each of the bands consist of 5000 element silicon charge coupled detectors. Only 4000 of these detectors are used at any one time. A time lag of about 55 seconds occurs between the acquisition of the backward image and the nadir image. The stereo configuration is given with the setting angle of 27.60° between the nadir and the backward telescope.

The used ASTER Level 1B data are Level 1A data with the radiometric and geometric coefficients applied. The L1B data are provided in a HDF file, together with the necessary metadata like longitude, latitute and exact acquisition times of each pixel.

2.1.3 Cloud-top height retrieval

To calculate the cloud-top height at each cloud pixel, corresponding image features have to be found with matching. Section 4 describes the main processing steps required for an effective cloud-adapted matching. The resulting y-parallaxes are then converted into cloud heights as:

$$CTH = \frac{y_p}{\tan(q_{frwd}) - \tan(q_{nadir})} \qquad (1)$$

with y_p: along-track parallax; considering that the zenith angles have to be projected on the along-track plane.

The height values of the successfully matched points are interpolated to the full 512x512 (ATSR2) or 4980x4200 (ASTER) grid.

2.1.4 Across-track wind retrieval and along-track wind error

The forward and nadir ATSR2 (ASTER) images are acquired with a mean time delay of 120 (55) seconds so that significant cloud motion is observable between the two scans. Given no time delay, the following relationships are fulfilled:

$x_p = 0$

$$y_p = CTH * [\tan(q_{frwd}) - \tan(q_{nadir})] \qquad (2)$$

Considering time delay and cloud motion, equation (2) has to be modified as:

$x_p = ¦$(cross-track wind) (3)

$y_p = ¦$(CTH, θ_{frwd}, θ_{nadir}, along-track wind)

For the cross-track wind retrieval and along-track wind correction, the exact time difference between the corresponding pixels in the forward and the nadir scan is calculated from the along-track distance on the ground and the satellite velocity. For the conical scanning of ATSR2, the time difference varies significantly across the scan.

North winds lead to an underestimation of the heights so that the along-track wind component has to be added to the y-parallax while southerly winds result in too high cloud-top heights.

As horizontal wind and cloud motion do not necessarily correspond, especially over mountainous terrain, it is not recommended to use wind data (e.g. from NWP model output) for the cloud motion error correction. A more reliable method is the use of cloud

tracking information from geostationary satellites, as we showed in Seiz and Baltsavias (2000); over Switzerland, there are the following three possibilities:

- Meteosat-6 5min Rapid Scans: during the Mesoscale Alpine Programme (MAP) in autumn 1999 (Sep – Nov) (EUMETSAT 2002).
- Meteosat-6 10min Rapid Scans: since September 2001, an operational 10min Rapid Scanning Service (RSS) is maintained (EUMETSAT 2002).
- The operational European meteorological geostationary satellite, Meteosat-7 (EUMETSAT, 2002).

The disadvantage of the Meteosat-7 images against the 5min or 10min Meteosat-6 Rapid Scans is the increased difficulty to assign the Meteosat cloud motion to the corresponding cloud objects within the ATSR2 stereo pairs. Furthermore, the tracking is more difficult as the shape of the clouds can change significantly within the 30min interval.

For the ATSR2 and ASTER CTH wind correction, the extracted Meteosat-6 and Meteosat-7 motion vectors were resampled to the ATSR2 or ASTER grid, and the cross-track and along-track components calculated. With the time difference between nadir and forward acquisition, the along-track components are converted into the CTH correction amounts.

2.2 Multi-view polar-orbiting satellite

2.2.1 MISR

As an alternative to the logistically difficult problem of a tandem mission of two polar-orbiting satellites to get synchronous high-resolution stereo images, the use of at least three non-symmetric views from a single polar-orbiting satellite can solve the issue of cloud motion errors in satellite-based stereo CTHs, as it allows the simultaneous estimation of CTH and CTW. The only currently operational satellite to offer such multi-view stereo images is the Multi-angle Imaging SpectroRadiometer (MISR). MISR was launched aboard the EOS AM-1 Terra spacecraft in December 1999. The orbit is sun-synchronous at a mean height of 705km, with an inclination of 98.5 and an equatorial crossing time at about 10:30 am. The repeat cycle is 16 days. The MISR instrument consists of nine pushbroom cameras at different viewing angles: -70.5° (named DA), -60.0° (CA), -45.6° (BA), -26.1° (AA), 0.0° (AN), 26.1° (AF), 45.6° (BF), 60.0° (CF), and 70.5° (DF). The time delay between adjacent camera views is 45-60 seconds which results in a total delay between the DA and DF image of about 7 minutes. The four MISR spectral bands are centered at 446 (blue), 558 (green), 672 (red), and 866 nm (NIR). The data of the red band from all nine cameras and of the blue, green and NIR bands of the AN camera are saved in high-resolution, with a pixel size of 275 x 275 m; the data of the blue, green and NIR bands of the remaining eight cameras are stored in low-resolution , with a pixel size of 1.1 x 1.1 km. The operational data products from NASA are described in Lewicki et al. (1999); the two products used for our investigations so far are the L1B2 Ellipsoid data (geolocated product) and the L2TC data (top-of-the-atmosphere/ cloud product). With the development of a general sensor model for linear array sensors, we will start directly with the L1B1 data (unrectified product) in the near future (Poli, 2002).

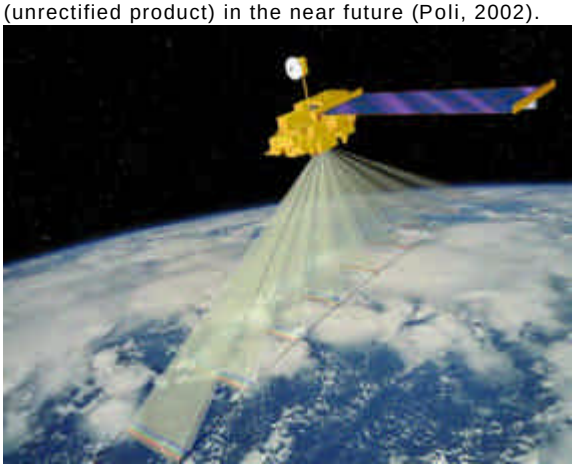

Figure 1. Multi-angle Imaging SpectroRadiometer (MISR).

2.2.2 Cloud-top height and motion retrieval

Stereo CTH on a 1.1 x 1.1 km grid and CTW on a 70.4 x 70.4 km grid are provided within the operational MISR processing chain as part of the level 2TC product. The algorithms applied for the CTH and CTW retrieval are described in Diner et al. (1999) and Horvath and Davies (2001). Important to note is that no subpixel matching algorithm is used and that the CTH and CTW for the high-resolution 1.1 x 1.1 km CTH product are not retrieved simultaneously, but in two steps: first, camera triplets (AN-BF-DF and/or AN-BA-DA) determine two CTW values for each 70.4 x 70.4 km with a histogram analysis; second, the matching results of AN-AF and/or AN-AA are converted into CTH and corrected with the amount due to cloud motion within the 45 s between the acquisition of the two views. So, the principle of the algorithm is finally similar to our combined ATSR2-Meteosat-6 approach, except that only one instrument has to be used for the retrieval. The disadvantage in our approach with using two different satellites is obviously that the cloud objects can be slightly different in shape, so that the height correction is not applied correctly for example at the cloud borders. Furthermore, differences in the wavelengths of the spectral channels used can also lead to errors in the correction, especially for multi-layer cloud situations. The disadvantage of the operational L2TC approach is that large discontinuities in the sparse CTW field can have a significant effect on the quality of the L2TC StereoHeight product, even if the AN-AF (and/or AN-AA) matching for their retrieval is very accurate and reliable. The MISR L2TC StereoHeight product can thereby suffer from some sort of blocking within the results. The 70.4 x 70.4 km CTW grid is probably too sparse, especially over land and mountainous terrain.

It is very likely that the wind field is not homogenous within such a large grid cell, and as consequence, the CTH field is not accurately corrected. Another important factor for the quality of the CTW field and consequently the CTH field is the matching method. Operationally, the so-called NM matcher (Diner et al., 1999) is used for getting the triplets in the first step; only in the second step, the more reliable M23 matcher is applied. Some matching tests on this dataset have shown that, with applying the M23 matcher for both steps, the CTW results and the blocking problem can be improved significantly. Another possibility is an increase of the spatial resolution from 70.4 km to 35.2 km (Horvath et al., 2002).

As own investigation, we started with the rectified MISR L1B2 Ellipsoid data, to test the LSM matching at this higher spatial resolution of 275 m versus ATSR2 and to evaluate if pixel-based triplet matching is possible with sufficient accuracy. After the multi-patch matching (see Section 4), the resulting x- and y-parallaxes from three non-symmetric views (e.g. AN-AA-CF) are converted into CTH, along-track and cross-track wind components with the linear equations described in Diner et al. (1999). In the equations, the zenith angles from the Ancillary Geometric Product and the coefficients provided in the L1B2 metadata to calculate the exact acquisition time of each pixel are used. Especially between non-adjacent cameras, the matching is more difficult and will require some adaptations of the LSM algorithm to deal with shape changes and appearance/disappearance of cloud features. In particular the DF view is very delicate to be matched with the other views (Fig. 4); additionally, it is more problematic to assume that there is no vertical motion within 3.5 min (AN-DF) than within 45 s (AN-AF) or 92 s (AN-BF). With our current version of the LSM matching, the use of the AN, AF, BF and CF views (to profit from the reliable sub-pixel accuracy of the matcher) seems to give better results, even if the separability of the parallax due to cloud height and the parallax due to cloud motion is mathematically better with including the most oblique viewing angle(s) in the triplet (see Horvath and Davies, 2001, determinants of linear equation system for the different camera triplet combinations).

2.3 Geostationary stereo view: Meteosat-6/ Meteosat-7

The Meteosat-6 5min Rapid Scans during MAP together with the images from the operational Meteosat-7 satellite provided the possibility to stereo-view clouds over Europe with a geostationary satellite for the first time (Seiz and Baltsavias, 2000). As the Meteosat satellites have a reversed scan mode (south-north) with respect to all other meteorological satellites, their images cannot be used for stereo mapping with other geostationary satellites. The first stereo configuration with two Meteosat satellites in general was achieved with Meteosat-5 and Meteosat-7 over the Indian Ocean, since the Meteosat-5 satellite was placed at 63 E for the INDOEX project (Campbell and Holmlund, 2000).

Unfortunately, the stereo configuration of Meteosat-6 and Meteosat-7 over Europe cannot be used for quantitative stereo analysis due to three reasons:

- Small longitude difference: Due to the small longitude difference of the two satellites, 0 and 9 W, compared to the satellite height, the base-to-height ratio is unfavorably low (~ 0.18).
- Scan synchronization: The two satellites are not synchronized, so that it is difficult to reach subpixel accuracy with matching, including the necessary motion correction. For the Meteosat-6 5min Rapid Scans, the time difference was about 1min, while for the new Meteosat-6 10min configuration, the time difference is more than 5min.
- Low image resolution: Given the spatial resolution of 2.5 x 4 km over Switzerland, small matching inaccuracies lead already to rather large CTH errors, which is even enhanced with the low base-to-height ratio.

3. GROUND-BASED STEREO ANALYSIS

Our newly developed ground-based stereo imager system (Fig. 2) (Seiz et al., 2002) was used for the stereo image acquisition of the cloud base. The imager system was part of the MAP-Special Observation Period (SOP) composite observing system which was set up at the Rhine Valley, Switzerland in autumn 1999. An improved version of the system is now installed at the Zürich-Kloten airport since September 2001.

Figure 2. Ground-based camera system.

Important prerequisite for accurate cloud-base height results from the camera system is a precise

determination of the interior and exterior orientation of the cameras. The interior orientation is determined with a close-range photogrammetric test field at our institute, before and after a measurement campaign. The exterior orientation is calculated based on star images during clear nights, with the camera locations measured with GPS. The calibration process is described in detail in Seiz et al. (2002).

4. CLOUD-ADAPTED MATCHING

To calculate cloud-base height (CBH) and cloud-top height (CTH) automatically, different image processing algorithms, especially image matching, have to be applied. In the following sections, these processing steps are explained in detail.

4.1 Preprocessing

As preprocessing, the images are usually contrast-enhanced and radiometrically equalized with a Wallis filter (Wallis, 1976). Wallis is an adaptive, local, nonlinear filter which is defined with the objective to force the mean and the contrast (or dynamic range) of an image to fit to some given target values.

4.2 Feature selection

Feature extraction is used to extract important image information, i.e. to supress redundant information or neglect information which is not used in the following processes. For the matching, the selection of distinct points and edges is important.

The Förstner interest operator (Förstner and Gülch, 1987) was used for extraction points with good texture. A point is selected if the windows' grey level signal ellipse is small and circular based on two thresholds.

4.3 Matching

As no a priori values of the cloud heights are given to the matching algorithm, a hierarchical matching procedure with multiple pyramid levels is applied so that the maximum possible parallax at the highest level is only 1-2 pixels. Every pyramid level is enhanced and radiometrically equalized with a Wallis filter. Points are selected with the Förstner interest operator (see 4.2) in the first pyramid level because it is likely that the same points are well detectable also in the other levels. The matching was done with the Multi-Photo Geometrically Constrained Matching Software package developed at our institute (Baltsavias, 1991), which is based on Least-Squares-Matching (LSM) (Grün, 1985). The matching solutions are quality-controlled with absolute and relative tests on the matching statistics.

When all the orientation parameters are known, as with our ground-based camera system, the matching algorithm can include geometric constraints. With the geometric constraints, the search space is restricted along the epipolar lines (Fig. 3).

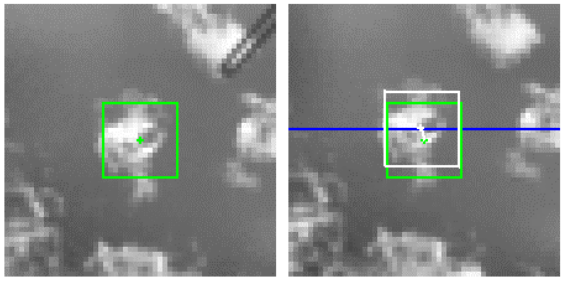

Figure 3. Illustration of geometrically constrained matching on a ground-based stereo pair. Left: template image; right: patch image (green: point approximation; white: matching solution; blue: epipolar line).

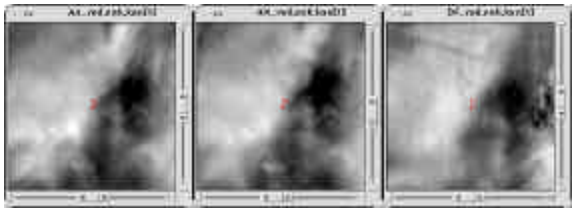

Figure 4. Matching difficulties with more oblique viewing angles of MISR (e.g. DF) versus matching between adjacent views (AA, AN).

5. RESULTS

For case 1, 13/10/1999 during MAP, with a mean cloud height of 10 km, an area of approximately 15 x 10 km can be used for the stereo-photogrammetric analysis of the images from the ground-based system (see Fig. 7). Table 1 shows the extracted ATSR2 CTH and Meteosat-6 cloud motion within the cameras' field of view. The retrieved mean height in this area is 11.3 km above sea-level from the 11.0 µm channel and 10.2 km from the 0.87 µm channel. Obviously, only the upper layer is seen in the 11.0 µm channel, while in the 0.87 µm channel, cloud points both in the lower and higher layer are detected. In the ground-based images, two layers of clouds are visible.

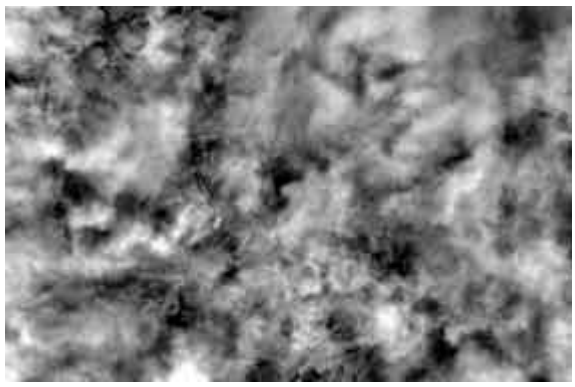

Figure 5. ASTER nadir image (enhanced) over Zuerich-Kloten, 12/04/2002.

Case 2, 12/04/2002 at Zuerich-Kloten, is a unique data set of coincident ASTER, MISR and ground-

based data. As ASTER was only scheduled on demand, such a coincidence is exceptional, especially regarding the nicely to analyze cloud situation. Figure 5 and 6 below show part of the ASTER image, over Zuerich-Kloten (resolution: 15m), and the ground-based image from the western camera. This unique data set will be used for assimilation tests with a very-high resolution version of the operational MeteoSwiss NWP model aLMo.

Figure 6. Ground-based image (enhanced) from camera 'west', 12/04/2002, 10:35:00 UTC, at ASTER overflight time.

6. CONCLUSIONS

This paper has shown examples of satellite- and ground-based stereo analysis of clouds. From satellites, there are various sensors currently which can be used for stereo-photogrammetric cloud retrievals. For Stereo CTHs from a single polar-orbiter with only two viewing angles (e.g. ATSR2, ASTER), it has proven to be absolutely necessary to correct the preliminary heights with CTW data from another source. Over land and mountainous regions, the cloud motion is most accurately derived from simultaneous images of a geostationary satellite. Over Europe, the Meteosat-6 Rapid Scan trials in 1999 (5min) and in 2000 (10min), and the operational Meteosat-6 10min Rapid Scans (since September 2001) are perfectly suited for this objective. The new MISR instrument and its products were presented, as a promising alternative to derive CTH and CTW simultaneously with stereo-photogrammetric methods. The images from our new ground-based imager system (skycam) showed to be valuable validation data for vertically thin cloud situations.

In Cloudmap2, the combined data sets will now be used for NWP assimilation tests on a very-high spatial resolution (MeteoSwiss aLMo model with 50 x 50m grid width) and for 3D modelling and visualization of the cloud situation.

ACKNOWLEDGEMENTS

The MAP data was provided by the various principal investigators of the MAP Rhine Valley target area and the Swiss Meteorological Institute. The Meteosat-6 and Meteosat-7 data were received from the EUMETSAT MARF Archive Facility, the ATSR2 data via the ESA ATSR2 NRT service, the EOS-Terra MISR data (level 1B2 and level 2TC) were obtained from the NASA Langley Research Center Atmospheric Sciences Data Center and the ASTER data were received from the Japanese ASTER User Service. We thank Catherine Moroney and Akos Horvath, JPL/ University of Arizona, for the reprocessing of the MISR L2TC dataset and for valuable input in the understanding of the L2TC products, Chris Hansen, EUMETSAT, for answers about the Meteosat-6 data, and the ASTER project team that the acquisition from ASTER succeeded in coincidence with our ground measurements. This work is funded by the Bundesamt für Bildung und Wissenschaft (BBW) within the EU-project CLOUDMAP2 (BBW Nr. 00.0355-1).

REFERENCES

ASTER, 2002. Project homepage at JPL: http://asterweb.jpl.nasa.gov.

Baltsavias, E.P., 1991. Multiphoto Geometrically Constrained Matching. Ph. D. dissertation, Institute of Geodesy and Photogrammetry, ETH Zurich, Mitteilungen No. 49, 221 p.

Campbell, G.C., Holmlund, K., 2000. Geometric cloud heights from Meteosat and AVHRR, Proceedings Fifth International Winds Workshop, EUMETSAT, EUM P28.

CLOUDMAP2, 2002. Projekt-Homepage: http://www.ge.ucl.ac.uk/research/cloudmap2/cloudmap2.html

EUMETSAT, 2002. http://www.eumetsat.de/ → Rapid Scan Service (RSS).

Förstner, W., Gülch, E., 1987. A fast operator for detection and precise location of distinct points, corners, and centers of circular features. Proc. ISPRS Intercommission Conf. on Fast Processing of Photogrammetric Data, Interlaken, Switzerland, 2-4 June, pp. 281-305.

Fujita, T.T., 1982. Principle of stereoscopic height computations and their applications to stratospheric cirrus over severe thunderstorms, J. Met. Soc. Japan, 60, 1, pp. 355-368.

Grün, A., 1985. Adaptive least squares correlation: a powerful image matching technique. S. Afr. J. of Photogrammetry, Remote Sensing and Cartography, 14 (3), pp. 175-187.

Hasler, F., 1981. Stereographic observations from geosynchronous satellites: an important new tool for the atmospheric sciences, Bull. Am. Met. Soc., 62, 2, pp. 194-212.

Horvath, A., Davies, R., 2001. Feasibility and error analysis of cloud motion wind extraction from near-simultaneous multiangle MISR measurements, J. Atmos. Ocean. Technology, 18, April, pp. 591-608.

Horvath, A., Davies, R. and Seiz, G., 2002. Status of MISR cloud-motion wind product. 6th International

Winds Workshop, May 7-10, 2002, Madison, Wisconsin.

Lewicki, S., Chafin, B., Crean, K., Gluck, S., Miller, K., Paradise, S., 1999. MISR Data Products Specifications. NASA JPL, http://eosweb.larc.nasa.gov/PRODOCS/misr/readme/dps_ne_icd.pdf

Mutlow, Ch., 1999. ATSR-1/2 User Guide, Issue 1.0, Rutherford Appleton Laboratory.

Poli, D., 2002. General model for airborne and spaceborne linear array sensors. International Archives of Photogrammetry and Remote Sensing, Denver, CO, Vol. 34, Part B1 (in press).

Seiz, G., Baltsavias, E.P., 2000. Satellite- and ground-based stereo analysis of clouds during MAP, EUMETSAT Conference Proceedings, Bologna, pp. 805-812.

Seiz, G., Baltsavias, E.P., Grün, A., 2002. Cloud mapping from the ground: use of photogrammetric methods. Photogrammetric Engineering & Remote Sensing (PE&RS), 68 (9).

Wallis, R., 1976. An approach to the space variant restoration and enhancement of images. Proc. of Symp. on Current Mathematical Problems in Image Science, Naval Postgraduate School, Monterey CA, USA, November.

Yi, H., Minnis, P., Nguyen, L., Doelling, D.R., 2001. A proposed multiangle satellite dataset using GEO, LEO and Triana, AMS, 11th Conference on Satellite Meteorology and Oceanography 15 - 18 October, Madison, Wisconsin.

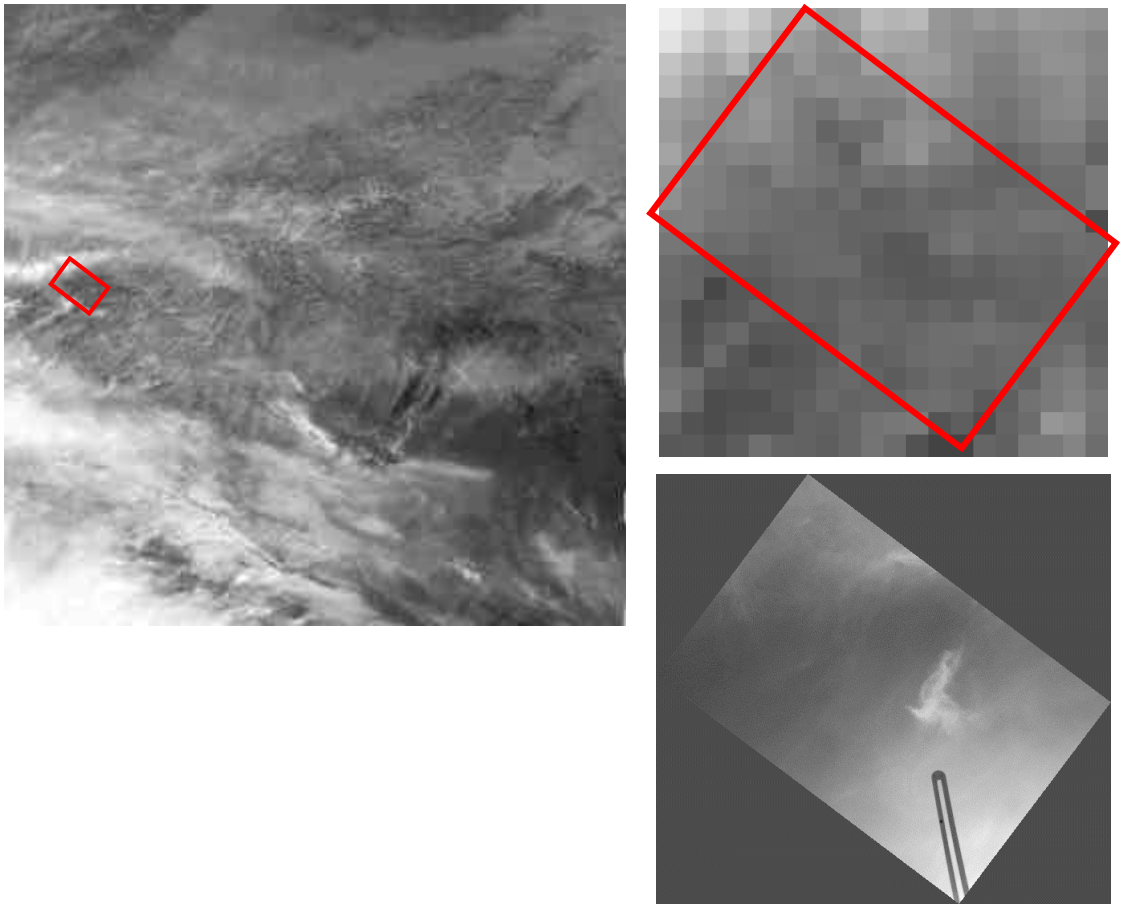

Figure 7. ATSR2 image, 11.0 µm channel (left; zoom: top right) and skycam image (bottom right) at Rhine Valley, Switzerland, on 13th October 1999. The skycam stereo FOV corresponds to the red rectangle within the ATSR2 image, approximately 14 x 9 pixels.

	ATSR2	**Meteosat-6**	**Skycam**	
			Lower layer	Upper layer
Height [km asl]	0.87 µm: 10.2 ± 0.7 [1] 11.0 µm: 11.3 ± 0.2 [1]	-	8.0 ± 0.11	10.9 ± 0.13
Motion [m/s]	-	19.3 [2]	17.8	25.8
Motion direction[ ]	-	275 [2]	274	276

Table 1. Cloud parameters derived over/ at Rhine Valley on 13th October 1999, from ATSR2, Meteosat-6 and the ground-based imager system (skycam). [1] within box of 20 x 20 pixels; [2] within box of 8 x 5 pixels.